Chemistry & Biology
Article

Supramolecular Iron Cylinder with Unprecedented DNA Binding Is a Potent Cytostatic and Apoptotic Agent without Exhibiting Genotoxicity

Anna C.G. Hotze,[1,3] Nikolas J. Hodges,[2,3] Rachel E. Hayden,[2,3] Carlos Sanchez-Cano,[1] Christopher Paines,[2] Natalia Male,[2] Man-Kit Tse,[2] Chris M. Bunce,[2,*] J. Kevin Chipman,[2,*] and Michael J. Hannon[1,*]
[1]School of Chemistry
[2]School of Biosciences
The University of Birmingham, Edgbaston, Birmingham B15 2TT, UK
[3]These authors contributed equally to this work
*Correspondence: c.m.bunce@bham.ac.uk (C.M.B.), j.k.chipman@bham.ac.uk (J.K.C.), m.j.hannon@bham.ac.uk (M.J.H.)
DOI 10.1016/j.chembiol.2008.10.016

SUMMARY

The supramolecular iron cylinder, $[Fe_2L_3]Cl_4$ (L = $C_{25}H_{20}N_4$), shows unprecedented DNA binding in vitro, inducing intramolecular DNA coiling and also targeting Y-shaped DNA junctions. We investigated its effects on proliferation and survival in both tumor and normal cell lines. Iron cylinder reduced mitochondrial activity of cultures with potency similar to cisplatin, inhibited the cell cycle, and increased cell death by apoptosis. Associated with this, we observed a lowering of the association of propidium iodide with cellular DNA consistent with an observed competitive displacement of PI from naked DNA by cylinders. Importantly, and in contrast to existing anticancer drugs such as cisplatin, the iron cylinder $[Fe_2L_3]^{4+}$ was not genotoxic. In summary, the design of metal complexes such as $[Fe_2L_3]^{4+}$ with potential anticancer properties in the absence of genotoxicity may represent a significant step toward therapeutic advancement.

INTRODUCTION

Agents that bind to DNA have the potential to control gene expression in cells and organisms (Dervan, 2001; Nielsen, 2001; Thuong and Helene, 1993; Da Ros et al., 2005; Hannon, 2007a). Potential applications include the ability to regulate a specific gene through binding of an agent with exclusive sequence or structure specificity. Less specific binding can also find application, and indeed a number of DNA binding agents of low specificity are in widespread clinical use for treating cancers and viral diseases. Such drugs are commonly small synthetic molecules and include intercalators such as the anthracycline antibiotics (for example adriamycin) used to treat cancers (Martínez and Chacón-García, 2005), minor-groove binders such as the synthetic diarylamidines berenil and pentamidine which are used to treat sleeping sickness (Baraldi et al., 2004), and the anticancer metallo drug cisplatin which acts via coordinative binding to two neighboring guanine bases of DNA, resulting in kinks in the DNA (Takahara et al., 1995; Reedijk, 1996; Lippert, 1999; Guo and Sadler, 2000; Hannon, 2007b).

We have pioneered the use of supramolecular chemistry to design synthetic agents which are of similar size and shape to the protein motifs used in nature to recognize DNA (Hannon et al., 2001a; Meistermann et al., 2002). In particular, we have designed metallo-supramolecular cylinders which are of a similar size (approximately 2 nm in length and 1 nm in diameter) and shape to the zinc finger motifs found in certain DNA-recognition proteins. These synthetic supramolecular cylinders bear a tetracationic charge and are composed of three ligand strands wrapped about two metal ions to give an $[M_2L_3]^{4+}$ formulation (Hannon et al., 2001a, 2001b; Meistermann et al., 2002; Kerckhoffs et al., 2007). The cylinders are the correct size and shape to fit into the B-DNA major groove spanning across about five base pairs, but are too large to bind in the minor groove (Hannon et al., 2001a; Meistermann et al., 2002; Moldrheim et al., 2002; Khalid et al., 2006). Although the cylinders may be designed with a variety of different metal ions, the main focus of our DNA binding studies has been the di-iron (II) cylinder $[Fe_2L_3]^{4+}$, $[Fe_2(C_{25}H_{20}N_4)_3]Cl_4$ (Figure 1), which has a deep purple color which provides a useful spectroscopic handle to follow its binding. This synthetic tetracationic supramolecular cylinder binds strongly (binding constant $>10^7$ M^{-1}) and noncovalently to the major groove of DNA and induces dramatic and unexpected intramolecular DNA coiling that is unprecedented with synthetic agents and somewhat reminiscent of the effect of histones (Hannon et al., 2001a; Meistermann et al., 2002). Although that coiling appears to be a consequence of major-groove binding, very recently it has been established by X-ray crystallography and NMR that this agent can also bind to DNA in a second mode: at the heart of a Y-shaped DNA three-way junction (Oleksi et al., 2006; Cerasino et al., 2007; Malina et al., 2007). Such a mode of DNA recognition is without precedent. Given the remarkable and unprecedented DNA binding properties of the cylinder, we were intrigued to explore the effect of these supramolecular cylinders on biological cells.

It is particularly instructive to consider this compound in the light of the cisplatin $[PtCl_2(NH_3)_2]$ family of drugs (cisplatin, carboplatin, nedaplatin, and oxaliplatin), which are among the leading anticancer drugs in the clinic and are the archetypal metal-based drugs (Takahara et al., 1995; Reedijk, 1996; Lippert, 1999; Guo and Sadler, 2000; Hannon, 2007b). These platinum drugs are

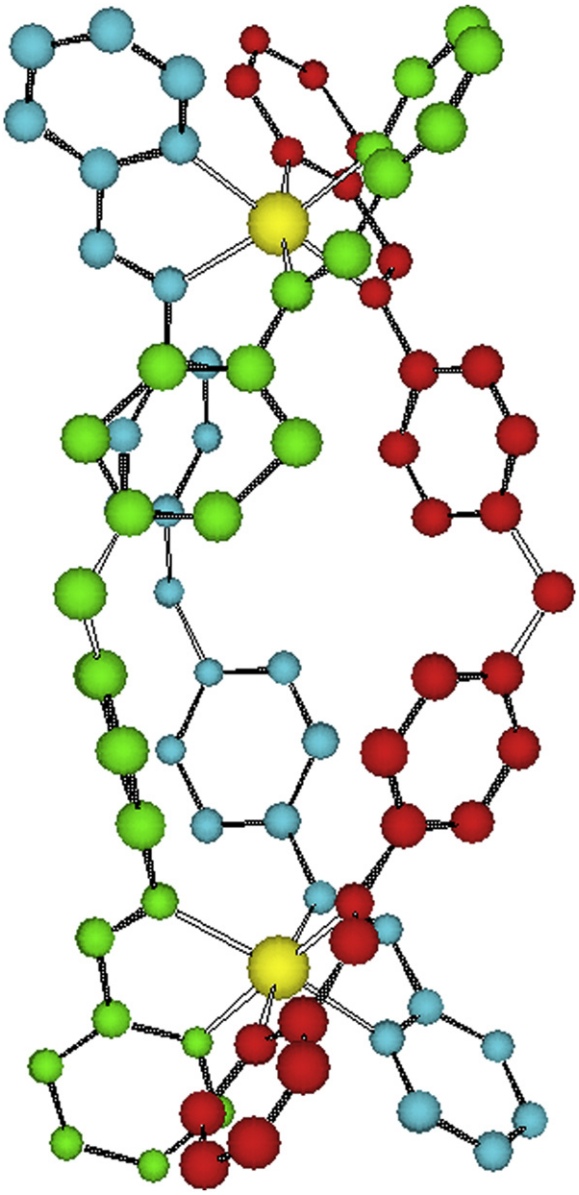

Figure 1. Molecular Structure of the Supramolecular Iron Cylinder Tetracation

$[Fe_2L_3]^{4+}$ hydrogens and chloride counter ions are omitted for the sake of clarity (structural data; Kerckhoffs et al., 2007; Cambridge Crystallographic Database 622770).

quite small molecules that act by forming metal-nitrogen bonds to the N7 positions of DNA purine bases. Ultimately, this leads to DNA damage, mutations, and lesions that cannot be repaired. In contrast, the supramolecular cylinders are not only much larger in size but also lack the presence of available coordination sites on the metals. They are thus unable to bind by formation of metal-nitrogen bonds to the DNA and instead bind through noncovalent interactions. Therefore, we anticipated that this supramolecular iron cylinder, $[Fe_2L_3]^{4+}$, might have quite different biological effects from those of the platinum drugs.

In the current study, we demonstrate that the supramolecular cylinder $[Fe_2L_3]Cl_4$ (L = $C_{25}H_{20}N_4$) is a potent inhibitor of cellular proliferation in a panel of tumor cells and induces cytostasis and apoptosis in the myeloid leukemia cell line HL-60. Crucially, we report no evidence that the cylinder $[Fe_2(C_{25}H_{20}N_4)_3]Cl_4$ is genotoxic as assessed by either the Ames test or the Comet assay, indicating a nongenotoxic mechanism of action.

RESULTS

Design and Synthesis of the Iron Cylinder $[Fe_2L_3]^{4+}$

The iron(II) cylinder $[Fe_2L_3]^{4+}$ is prepared in high yield by warming the ligand and iron(II) chloride in a 3:2 ratio in methanol solution for a few hours. The design of organic ligand L is such that two bidentate metal binding sites are separated by a 1,4-diphenylmethane spacer. The spacer prevents the two metal binding sites from binding to the same metal, and a dinuclear complex results. With a metal ion such as iron(II) which prefers a six-coordinate octahedral coordination geometry, three such binding sites are required to complete the coordination sphere of the metal. The programmed outcome is a dimetallic structure with three organic ligand strands wrapping around the dimetallo core. The cylinder bears a tetracationic charge (arising from the two iron[+2] centers) and can be isolated with a variety of counterions, with the choice of counterion influencing the solubility. The hexafluorophosphate salt affords good solubility in organic solvents (but not aqueous or alcoholic solvents), whereas the chloride salt has good water solubility and is used for the biological studies herein. The electrospray mass spectra of the salts confirm the expected 2:3 M:L stoichiometry with peaks corresponding to $\{Fe_2L_3\}^{4+}$ and $\{Fe_2L_3X\}^{3+}$ (X = PF_6, Cl). The iron(II) centers are low spin and the salts are consequently diamagnetic and are deep purple in color due to intense metal to ligand charge transfer transitions in the visible region. The NMR spectra confirm the presence of a single solution species of high symmetry. An X-ray crystal structure of the hexafluorophosphate salt of this iron cylinder confirms the triple-stranded helical nature of the cation (Kerckhoffs et al., 2007; ccdb 622770). The formation of such triple-stranded metallo-supramolecular structures (termed triple-helicates) is well established (Childs and Hannon, 2004), although the iron cylinder differs from many such arrays in the rigidity of its cylindrical structure. Alongside the metal-ligand interactions holding the three strands together, the aryl rings at the center of the cylinder form face-edge π-stacking interactions with each other in two groups of three, such that within a group of three each ring presents a face to a ring on one neighboring strand and an edge to a ring on the other neighboring strand. The consequences of this are two-fold. (1) The cylinder structure is supported by interactions along its length giving rise to a relatively rigid structure (this contrasts with other triple-helicates, where binding sites are more usually linked by flexible and floppy alkyl chains; Kramer et al., 1993). (2) The aryl rings are oriented about the metal-metal axis (rather than perpendicular to it as in Charbonniere et al., 1998), giving rise to the cylindrical or barrel-shaped structure. The structure of the iron(II) cylinder $[Fe_2L_3]^{4+}$ is not only distinct from other helicates but quite different in size and shape from other multimetallic DNA binders such as diruthenium bis-intercalators which contain two bulky metal centers linked through just one strand (directly or via a floppy spacer; Lincoln and Nordén, 1998; Önfelt et al., 2002) and the polynuclear

Table 1. IC_{50} Concentrations (μM) of Iron Cylinder $[Fe_2L_3]Cl_4$ and Cisplatin in a Panel of Cell Lines as Assessed by the MTT Assay

	HBL100	T47D	SKOV3	HL-60	MRC5
Iron cylinder	27 ± 5	52 ± 10	35 ± 5	18 ± 3	19 ± 3
Cisplatin	4.9 ± 0.3	28 ± 1.7	6 ± 0.3	7 ± 1	<3

See Experimental Procedures. Cells were treated for 72 hr with iron cylinder (0–129 μM) or cisplatin (0–100 μM). The results represent the mean of three separate experiments ± SD (n = 3).

Table 2. Lack of Induction of DNA Strand Breaks following Cylinder Treatment as Assessed by the Alkaline Comet Assay

Iron Cylinder (μM)	MRC5	HBL100	HL-60
0	1.43 ± 0.82	4.89 ± 3.84	0.27 ± 0.15
5	2.18 ± 0.12	8.93 ± 4.07	0.40 ± 0.51
10	2.54 ± 0.47	6.16 ± 4.41	0.39 ± 0.47
15	2.31 ± 0.57	6.29 ± 4.17	0.45 ± 0.39
20	1.86 ± 0.44	6.48 ± 2.46	1.95 ± 2.33
25	2.32 ± 0.22	ND	ND

The results represent tail DNA % ± SD (n = 3) of three independent experiments. There was no statistically significant effect of cylinder treatment (24 hr) at any of the concentrations investigated in any cell line studied. ND, not determined because 25 μM, 24 hr was toxic to these cell lines.

platinum compounds composed of metals linked by long floppy alkyl chains (Komeda et al., 2006). It is the size and shape of the iron cylinders (both of which are inherent consequences of their supramolecular architecture) that give rise to their dramatic and unprecedented DNA binding properties as illustrated by the crystal structure of an iron cylinder in complex with a DNA three-way junction in which the cylinder fits perfectly into the heart of the DNA junction without significant structural perturbation (Oleksi et al., 2006).

Relative Effects of Iron Cylinder $[Fe_2L_3]^{4+}$ on Mitochondrial MTT Reduction

The iron cylinder $[Fe_2L_3]^{4+}$ inhibited 3-(4,5-Dimethylthiazol-2-yl)-2,5-diphenyltetrazolium bromide (MTT) mitochondrial activity at low micromolar concentrations in the nontumor MRC5 and tumor HBL100, SKOV3, T47D, and HL-60 cell lines shown in comparison to cisplatin (Table 1). This inhibition may indicate a direct toxicity to cellular mitochondria but can also be indicative of reduced cell number by cell death or by inhibition of growth (see below).

No Evidence for Cylinder-Related Genotoxicity

When tested up to concentrations cytotoxic to bacteria, the iron cylinder $[Fe_2L_3]^{4+}$ was negative in the Ames bacterial mutagenicity test either with or without metabolic activation by S9 using either TA98 or TA100 strains of *Salmonella typhimurium*. These strains are used to detect frameshift and point mutations, respectively (Maron and Ames, 1983). The iron cylinder $[Fe_2L_3]^{4+}$ was tested at 8, 16, and 32 μM (higher concentrations were toxic to the bacteria) and the maximum number of bacterial revertants observed were 16 ± 6 (no S9) and 18 ± 3 (+S9) compared to 13 ± 4 (no S9) and 18 ± 4 (+S9) for controls in the TA98 strain. Similarly, values of 137 ± 14 (no S9) and 146 ± 17 (+S9) compared to 123 ± 3 (no S9) and 135 ± 9 (+S9) for controls in the TA100 strain also indicated a lack of mutagenicity of the iron cylinder. To investigate possible cylinder-related genotoxicity in mammalian cell lines, we investigated whether iron cylinder treatment could cause DNA strand breaks utilizing the Comet assay. There was no evidence that the iron cylinder treatment (0–25 μM, 24 hr) causes DNA strand breaks in HBL100, MRC5, or HL-60 cell lines under these experimental conditions (Table 2). In addition, there was also no evidence for DNA strand breaks in the SKOV3 cell line (data not shown).

Iron Cylinder Inhibits Cellular Proliferation and Causes Apoptosis

Treatment of cultures with iron cylinder $[Fe_2L_3]^{4+}$ resulted in inhibition of cell growth, and concentrations as low as 7 μM almost completely arrested growth of cultures in all the cell lines investigated (HBL100, SKOV3, and MRC5). This potent cytostasis is shown in Figure 2. For comparison, cisplatin inhibited cellular proliferation at concentrations of 2.5–5 μM in the same cell lines (data not shown). To investigate the possible mechanism of growth inhibition, we investigated whether treatment with iron cylinder could alter the distribution of cells within the cell cycle. For technical reasons, we chose to use the leukemic cell line HL-60 which grows in suspension and is therefore more amenable to cell-cycle analysis. Concentrations of 10, 25, and 100 μM were tested over several time periods (24 and 48 hr). The 100 μM dose was directly cytotoxic and only necrotic cells were obtained (data not shown). At 24 hr in 10 μM treated cells, we observed an increased percentage of cells in G_1/G_0 from 40.0% ± 3.5% in controls to 64.7% ± 4.5% in treated cultures together with a reduction in the percentage of cells in S phase (22.8% ± 6% compared to 43.8% ± 7%) (n = 4 experiments; Figure 3A). The differences between control and treated cells were highly statistically significant ($p < 0.001$, t test). An accumulation in G_0/G_1 was not observed in cells treated with 25 μM iron cylinder $[Fe_2L_3]^{4+}$, although the reduction in S phase was maintained. In addition, the higher dose of 25 μM gave rise to the accumulation of significant numbers of sub-G1 events (Figure 3B), which is indicative of cells undergoing programmed cell death, apoptosis (Heffeter et al., 2006). To further investigate this, we used dual propidium iodide (PI) and annexin-V (AV) staining. AV binds to the surface of apoptotic cells. Cells initiating apoptosis but that remain viable exclude PI. Thus, cells that are $AV^{+ve};PI^{-ve}$ represent early apoptotic cells and double positives represent postapoptotic cells. Treatment with 25 μM iron cylinder $[Fe_2L_3]^{4+}$ resulted in a time-dependent accumulation of AV-positive cells. At 48 hr, 17.1% of cells were AV positive, which is in close agreement with the 23.4% sub-G1 events identified by cell-cycle analysis. The flow cytometry analyses of HL-60 apoptosis data were complemented by data obtained using adherent cell lines in the DNA diffusion assay (which measures DNA fragmentation as a critical stage of apoptosis), Using this assay, there was no evidence for apoptosis following treatment with cylinder for 24 hr (0–25 μM). However, following treatment for 48 and 72 hr, we observed a concentration-dependent increase in the percentage of apoptotic nuclei which was statistically significant at the 25 μM dose (Figure 4).

Of particular interest, associated with the cell-cycle arrest and induction of apoptosis, we observed a lowering of the intensity of the PI signal, indicating a reduced association with cellular

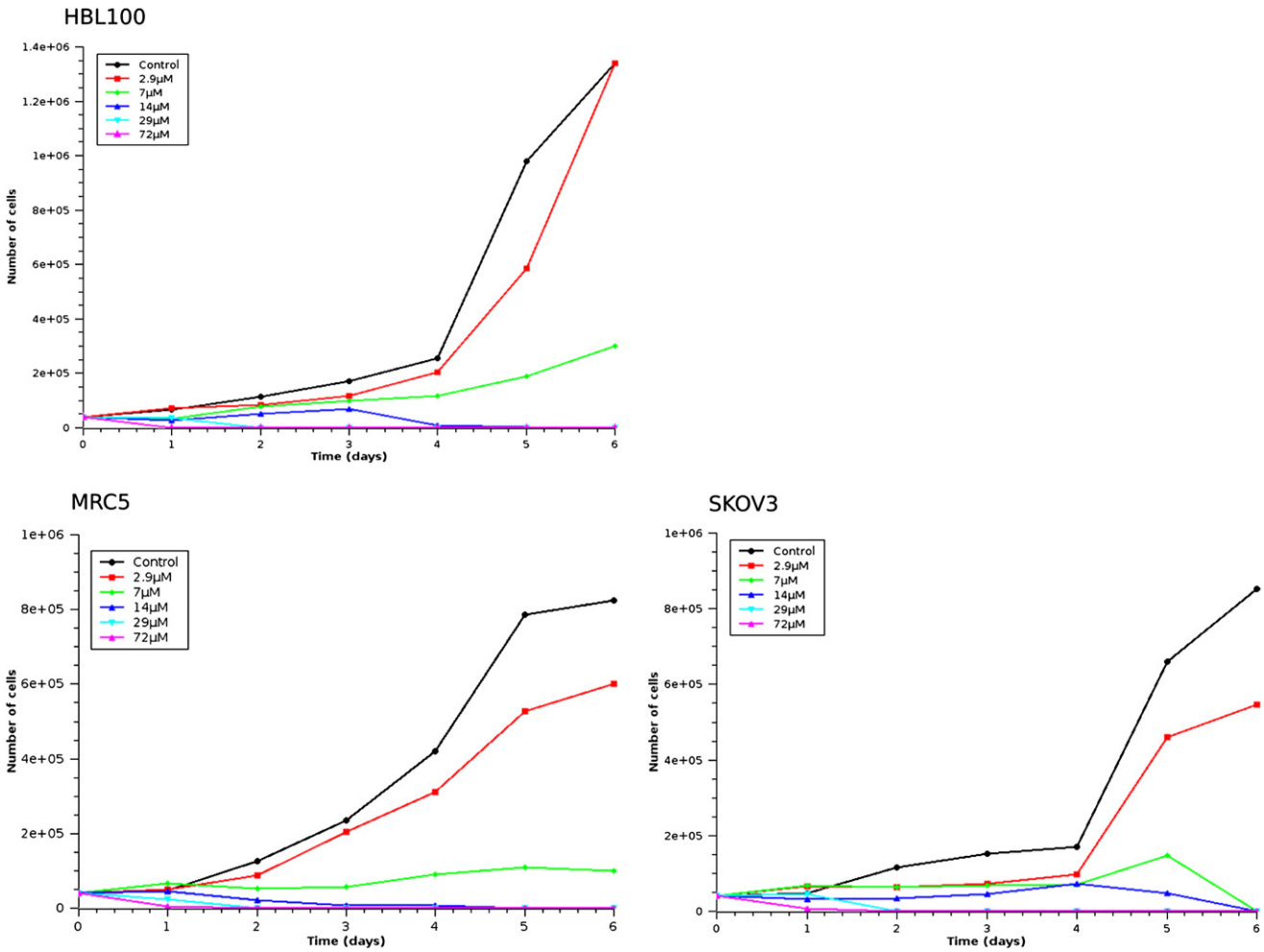

Figure 2. Inhibition of Cellular Growth by Iron Cylinder

After initial plating at a density of 40,000 cells per dish, cells were cultured in the continuous presence of iron cylinder (0–72 μM) for up to 6 days. Cell number per 35 mm dish was assessed every 24 hr using a hemocytometer as described in Experimental Procedures. The results represent the mean of three individual experiments repeated in duplicate (n = 3). Error bars plotting SD are omitted for the sake of clarity but were less than ±15% of the mean in all cases.

DNA (Figure 3B). We have previously shown that the cylinder displaces ethidium bromide from naked calf thymus DNA (Hannon et al., 2001a; Meistermann et al., 2002; Peberdy et al., 2007); in an analogous experiment it also displaces propidium iodide (Figure 5A). Therefore, the reduction in propidium fluorescence in the cellular assays indicates that the cylinder competes with binding on nuclear chromatin.

Hoechst Displacement Assay

As well as competitively displacing ethidium and propidium from DNA, the cylinder can displace other DNA binders, such as the Hoechst dyes, from naked DNA (Peberdy et al., 2007). Hoechst 33258 can also be used to stain DNA in live cells and thus in cellulo displacement may be probed. HL-60 cells were preloaded with the Hoechst dye (for 20 min) and then treated for 20 min with the cylinder, before being separated from the media, washed twice, and resuspended in PBS, and the Hoechst fluorescence was recorded. The Hoechst 33258 fluorescence signal decreases with increasing amount of cylinder (Figure 5B). This is consistent with the cylinder entering the cell and displacing Hoechst 33258 from cellular DNA as it does from naked DNA.

DISCUSSION

The iron(II) cylinders are an exciting new class of agents that act on DNA in completely different ways from the clinical drug cisplatin. In particular, the cylinder cannot only bind to the major groove of DNA (Hannon et al., 2001a; Meistermann et al., 2002; Moldrheim et al., 2002; Khalid et al., 2006) but it can also fit into three-way and other Y-shaped DNA junctions (Oleksi et al., 2006; Cerasino et al., 2007; Malina et al., 2007); Y-shaped junctions are found endogenously in cells in the form of DNA replication forks.

Importantly, when assessed by the endpoint of inhibition of cell growth, the potency of iron cylinder $[Fe_2L_3]^{4+}$ (approximately 7 μM) was broadly comparably to that of cisplatin (2.5–5 μM). In contrast, the IC_{50} values of the iron cylinder against several tumor cell lines, determined by an MTT assay of mitochondrial function in cultures, show an activity ranging from 18 to 57 μM which is, on

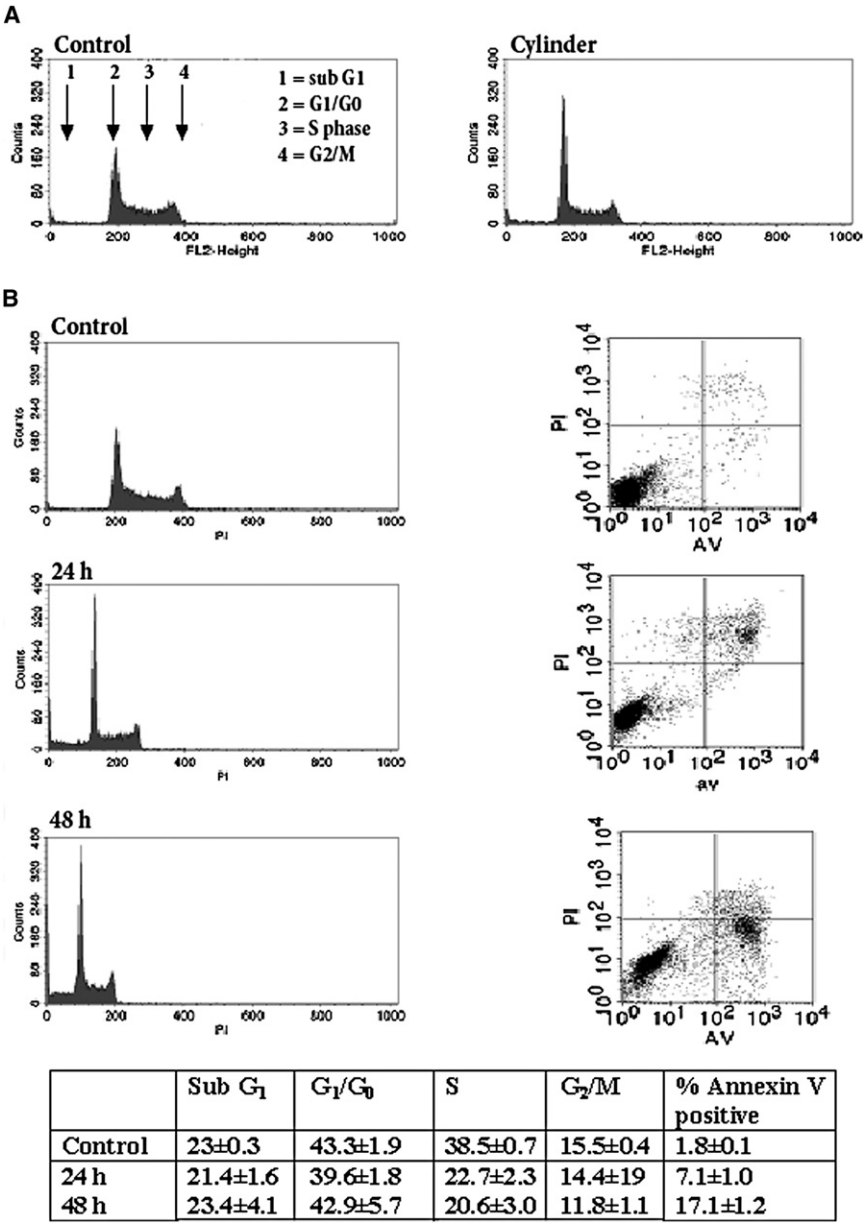

	Sub G_1	G_1/G_0	S	G_2/M	% Annexin V positive
Control	23±0.3	43.3±1.9	38.5±0.7	15.5±0.4	1.8±0.1
24 h	21.4±1.6	39.6±1.8	22.7±2.3	14.4±19	7.1±1.0
48 h	23.4±4.1	42.9±5.7	20.6±3.0	11.8±1.1	17.1±1.2

Figure 3. Disruption of Parameters Related to the Cell Cycle by Treatment with Iron Cylinder

(A) Induction of G_1 cell-cycle arrest following treatment with iron cylinder (10 μM, 24 hr) as assessed by propidium iodide staining of DNA and fluorescence activated cell sorting analysis. Plots are representative and mean values from n = 4 experiments are referred to in the text. Note the accumulation of cells in the G_1 phase of the cell cycle following treatment with iron cylinder $[Fe_2L_3]^{4+}$ (right panel) compared to control (left panel).

(B) Induction of apoptosis as assessed by flow cytometry and annexin-V staining at 24 and 48 hr following 25 μM cylinder. Left panels show a representative cell cycle for controls (top), 24 hr treatment (middle), and 48 hr (bottom). Right panels show annexin-V and propidium iodide staining at 24 and 48 hr following 25 μM treatment for control (top), 24 hr treatment (middle), and 48 hr (bottom). Cells below the horizontal bar are propidium iodide-negative (viable) cells. Cells to the right of the vertical line are annexin positive (apoptotic). The cells in the top right quadrant are late-stage apoptotic. The associated table shows the percentage of events in each stage of the cell cycle and the percentage of annexin-V-positive cells. N = 3 experiments ± SD.

average, in the cell lines tested approximately five times less than cisplatin. These results suggest that the molecular-level action of the iron cylinder is distinct from that of cisplatin and that whereas both agents are roughly equipotent cytostatic agents, cisplatin is more efficient at cell killing over the time course investigated. Interestingly, the MTT IC_{50} values obtained for the iron cylinder are more in the range of carboplatin, which is used as an alternative to cisplatin when there is a clinical need to minimize platinum drug side effects because of other medical conditions; carboplatin has a lower toxicity and subsequently fewer side effects (Lippert, 1999; Hannon, 2007b).

On the basis of our findings using a nontumor cell line (MCR5) as with cisplatin, we are not able to show a greater sensitivity of tumor cell lines to the cylinder; such potential selectivity would require further research. Interestingly, activity is seen in all the tumor cell lines tested in contrast to the analogous ruthenium(II) compound that is active in breast but not ovarian lines (Pascu et al., 2007).

The only other previous example of anticancer activity by structures with supramolecular architectures is our recent report of activity by dinuclear double-stranded ruthenium complexes (Hotze et al., 2006). Although one of these does have higher activity in cell lines than the cylinders herein, these cylinders combine a cylinder-like structure with "vacant" coordination sites which can potentially form direct metal-ligand bonds to the DNA bases, like cisplatin. The potential anticancer activity of metallo compounds that can bind only *noncovalently* to DNA has not been widely studied and has principally focused on platinum(II) and ruthenium(II) metallo intercalators rather than agents that address binding modes not currently employed by existing clinical drugs (Fisher et al., 2007; Wheate et al., 2007) (organic intercalators, such as doxorubicin, are currently used in the clinic for cancer treatment). For example, the simple Tris-chelate $[Ru(bpy)_3]^{2+}$, a groove binder, is reported to be inactive, although some related azopyridine-containing compounds with potential to (partially) insert between the bases do display some activity in cell lines (Hotze et al., 2005). Lincoln and Nordén (1998) have reported similar IC_{50} values to those herein for a dinuclear threading metallo intercalator based on ruthenium dppz units and whose DNA binding is distinct from that of simple intercalators. However, the agent is not active in

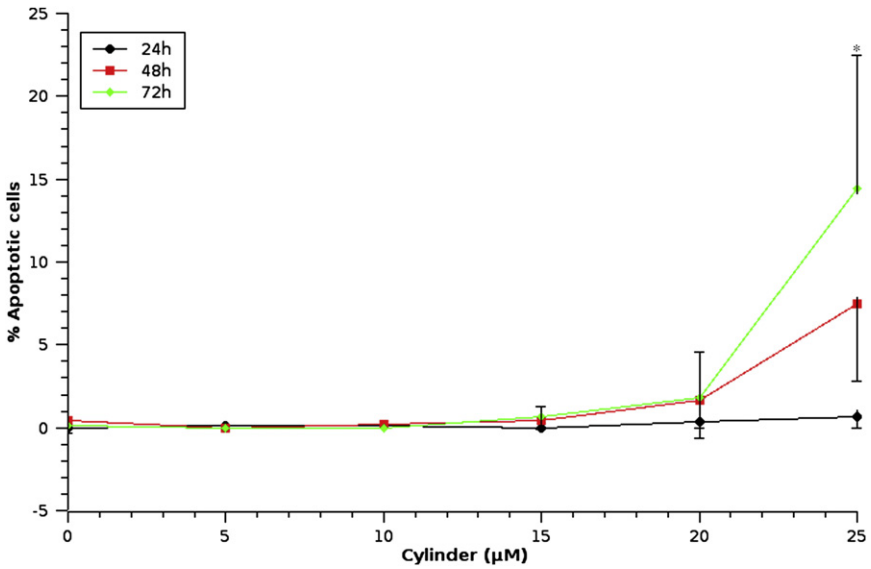

Figure 4. Induction of Apoptosis by Iron Cylinder $[Fe_2L_3]^{4+}$ as Assessed by the DNA Diffusion Assay

See Experimental Procedures. The results represent the mean of three experiments carried out in duplicate ± SD (n = 3). *, significantly different from untreated control, $p < 0.05$ (paired t test).

some other cell lines (Önfelt et al., 2002). Komeda et al. (2006) have very recently described a trinuclear platinum compound that binds noncovalently (through hydrogen bonds) to the DNA phosphate backbone in a mode that they describe as "phosphate clamping." Like the cylinders, this synthetic agent has a mode of binding to DNA that is not used by existing clinical DNA-targeting drugs. Like the cylinders, it also shows IC_{50} values in the micromolar range in cell lines (Harris et al., 2005a, 2005b).

What is particularly exciting is that our studies herein demonstrate the iron cylinder $[Fe_2L_3]^{4+}$ is not directly genotoxic using assays of base-pair or frameshift mutagenicity in bacteria and of DNA strand breaks in human cells. However, at this stage it is not possibly to completely exclude the possibility that the iron cylinder may cause mutations through indirect mechanisms such as inhibition of DNA repair. Many anticancer drugs, specifically cisplatin, covalently bind to DNA, induce oxidative stress, and cause DNA crosslinking and mutation (Uno and Morita, 1993; Gebel et al., 1997; Cohen and Lippard, 2001). The alkaline Comet assay was used to indicate whether direct DNA strand break formation might be involved in the mechanism of action of the iron cylinder. The Comet assay in intact cells showed that there was no indication of such DNA damage. These features (the lack of genotoxicity or mutagenicity) are important for potential drug design, and the results are in stark contrast to cisplatin and the other clinical platinum anticancer drugs which are genotoxic and potent mutagens. The potent genotoxity of cisplatin can result in the formation of secondary cancers (especially leukemias) as a result of cancer chemotherapy (Aung et al., 2002; Escudero et al., 2004; Wierecky et al., 2005), and therefore the design of metal complexes that have anticancer therapeutic properties but are not genotoxic or mutagenic would represent a significant advancement.

Cell-cycle studies in HL-60 cells treated with the iron cylinder $[Fe_2L_3]^{4+}$ (10 μM for 24 hr) showed a significant G_0/G_1 arrest and concomitant lowering of cell numbers in S phase. This dose did not induce significant apoptosis in either HL-60 or the adherent cell lines but was similar to that which led to cytostasis as measured in MTT assays (7 μM). The higher dose of 25 μM caused significant apoptosis both in HL-60 cells and adherent cells. An accumulation of G1 cells was not seen at this dose but a reduction in S phase remained. It is reasonable to suggest that these differences may relate to induced apoptosis occurring in G_0/G_1 cells, and further studies should address this. At 25 μM, iron cylinder treatment was associated with apparent binding of cylinder to cellular DNA, as evidenced by reduced DNA staining by PI in both cell-cycle and cytometry-based apoptosis assays. This was not as marked at 10 μM. Thus, the balance between mere G_0/G_1 arrest and the additional acquisition of apoptosis appears related to the extent of DNA binding. During chemotherapy, accumulation of cells in G_0/G_1 is as often the result of cell-cycle checkpoint activation as the result of DNA damage (Wang et al., 2008). In the case of the iron cylinder, because there is no cleavage of DNA, it is postulated that the noncovalent interaction of the compound with DNA may cause this cell-cycle arrest. It is the first time, to our knowledge, that a noncovalent and nongenotoxic interaction mode of a supramolecular iron complex with DNA is linked to an arrest of cells in the cell cycle. Beyond this G_0/G_1 arrest, we demonstrate herein, using two separate assays, that the mechanism of cell toxicity by the iron cylinder is through apoptosis. Although cellular senescence and cell death by necrosis are also important, sensitivity to apoptosis is known to be fundamental for therapeutic responses of malignant cells to chemotherapy including cisplatin treatment (Reedijk, 1996; Lippert, 1999). Modern drug design is often based on studies detecting the abilities of investigated complexes to induce apoptosis as the preferred mode of cell death because it avoids nonselective necrotic mechanisms that associate with adverse inflammatory responses (Fadeel and Orrenius, 2005).

Although the precise molecular basis of the cellular effects and toxicity of the iron cylinder $[Fe_2L_3]^{4+}$ remains to be fully elucidated, it is immediately clear from the studies herein that its activity and action are distinct from that of cisplatin and the other clinical platinum drugs that produce a range of DNA-damaging events contributing to mutation and cell death (Uno and Morita, 1993; Gebel et al., 1997; Cohen and Lippard, 2001). A mode of action that contrasts with that of cisplatin opens up the possibility of identifying anticancer treatment for disease with intrinsic and acquired resistance to agents such as cisplatin. On the basis of its known noncovalent DNA binding modes, one possible mechanism is that iron cylinder is able to bind to and stall DNA replication forks (a three-way junction structure). Whether the observed cell-cycle arrest is mediated by cell signaling pathways or more directly through the ability of the agent to coil, and

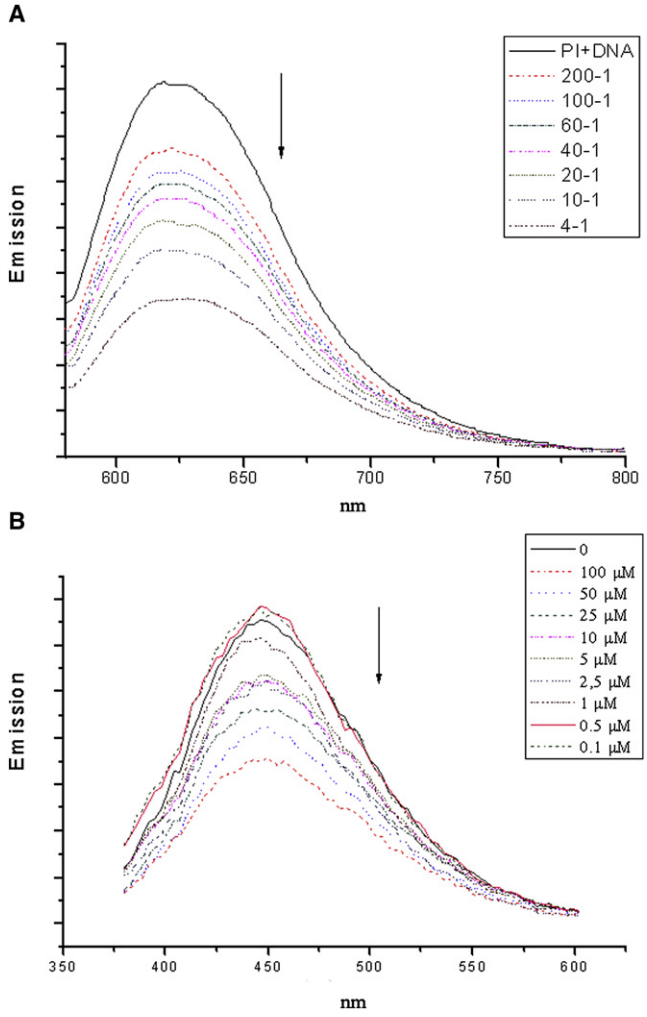

Figure 5. Iron Cylinder Displaces Fluorescent Probes from Both Purified and Cellular DNA

(A) Displacement of propidium iodide (1.5 μM) from ct-DNA (6 μM) by iron cylinder $[Fe_2L_3]^{4+}$. Mixing ratios Pi/cylinder are shown in the caption.

(B) Fluorescence displacement assay for HL-60 cells loaded with 10 μM Hoechst 33258 and then treated with varying concentrations of cylinder (concentrations indicated in the figure). λ_{exc} = 350 nm.

thereby lock away, regions of duplex DNA inhibiting gene expression is yet to be determined.

SIGNIFICANCE

In the current study, we have shown for the first time, to our knowledge, that a noncovalent and nongenotoxic interaction mode of a supramolecular iron complex with DNA is linked to an arrest of cells in the G_0/G_1 phase of the cell cycle and subsequent death through apoptosis. The design of metal complexes such as the iron cylinder $[Fe_2L_3]^{4+}$ with potential anticancer properties in the absence of genotoxicity may represent a significant step toward therapeutic advancement compared to traditional agents such as cisplatin which induce cell death through covalent modification to DNA and genotoxicity. Further research into the mechanism of action and potential application of iron cylinder and other cylinders based on other metals, such as the ruthenium(II) cylinder which also displays activity in cell lines (Pascu et al., 2007), is currently under way in our laboratories.

EXPERIMENTAL PROCEDURES

Synthesis

Ligand L: 2-pyridine carboxaldehyde (1.4 cm^3, 15.1 mmol) and 4,4′-methylenedianiline (1.5 g, 7.6 mmol) were stirred in ethanol (25 cm^3) at room temperature for 12 hr. The yellow solid that precipitated was collected by vacuum filtration, recrystallized from ethanol, and dried in vacuo (2.6 g, 84%).

Mass spectrum (= ve FAB): *m/z* 377 {M + H}.

Found: C, 79.4; H, 5.3; N, 14.7. Calculated for $C_{25}H_{20}N_4 \cdot 0.125H_2O$: C, 79.3; H, 5.4; N, 14.8%

^{1}H NMR ($CDCl_3$) (250 MHz) at 298K: δ 8.73 (2H, d, *J* = 4.0 Hz, H_6), 8.65 (2H, s, H_i), 8.23 (2H, d, *J* = 7.0 Hz, H_3), 7.83 (2H, td, *J* = 8.3, 1.9, 0.6 Hz, H_4), 7.39 (2H, ddd, *J* = 7.6, 4.9, 1.2 Hz, H_5), 7.29 (8H, m, H_{Ph}), 4.07 (2H, s, CH_2).

$[Fe_2L_3][PF_6]_4$: ligand L (0.0301 g, 0.08 mmol) and iron(II) chloride (0.0106 g, 0.05 mmol) were heated under reflux in methanol (20 cm^3) under dinitrogen for 2 hr. The resulting purple-colored solution was cooled and treated with saturated methanolic ammonium hexafluorophosphate. On cooling, a purple precipitate separated and was isolated by filtration (0.0408 g, 84%).

Mass spectrum (ESI): *m/z* 310 $\{Fe_2L_3\}^{4+}$ 100%, 421 $\{Fe_2L_3F\}^{3+}$ 1%, 462 $\{Fe_2L_3(PF_6)\}^{3+}$ 1%.

Found: C, 47.3; H, 3.3; N, 8.7. Calculated for $Fe_2C_{75}H_{60}N_{12}P_4F_{24} \cdot 4H_2O$: C, 47.6; H, 3.6; N, 8.9%

^{1}H NMR (CD_3CN) (400 MHz) at 233K: δ 8.75 (1H, s, H_i), 8.48 (1H, d, *J* = 7.4 Hz, H_3), 8.34 (1H, t, *J* = 7.4 Hz, H_4), 7.68 (1H, t, *J* = 6.4 Hz, H_5), 7.22 (2H, m, $H_{6,Ph}$), 6.55 (1H, d, *J* = 7.8 Hz, H_{Ph}), 5.75 (1H, d, *J* = 6.9 Hz, H_{Ph}), 5.17 (1H, d, *J* = 7.4 Hz, H_{Ph}) 3.98 (1H, s, CH_2).

UV/vis (MeCN): 524 (ε = 11,500), 572 (ε = 15,300) nm.

The chloride salt $[Fe_2L_3]Cl_4$ was prepared by an analogous route.

Mass spectrum (ESI): *m/z* 310 $\{Fe_2L_3\}^{4+}$ 100%, 425 $\{Fe_2L_3Cl\}^{3+}$ 40%.

Found: C, 63.0; H, 4.5; N, 11.6. Calculated for $Fe_2C_{75}H_{60}N_{12}Cl_4 \cdot 2.5H_2O$: C, 63.1; H, 4.6; N, 11.8%.

^{1}H NMR (D_2O) (300 MHz) at 298K: δ 8.89 (1H, s, H_i), 8.44 (1H, d, *J* = 7.7 Hz, H_3), 8.27 (1H, t, *J* = 7.7 Hz, H_4), 7.58 (1H, t, *J* = 6.6 Hz, H_5), 7.27 (1H, d, *J* = 5.5 Hz, H_6), 7.1 (1H, br, H_{Ph}), 6.6 (1H, br, H_{Ph}), 5.7 (1H, br, H_{Ph}), 5.3 (1H, br, H_{Ph}), 3.89 (1H, s, CH_2).

UV/vis (H_2O): 324 (ε = 32,900), 524 (sh), 574 (ε = 16,900) nm.

Selection of Cell Lines

We wanted to investigate the biological properties of the iron cylinder $[Fe_2L_3]^{4+}$ in a panel of tumor cell lines in comparison to the effects of cisplatin. HBL100 and T47D were selected as representative breast cancer lines that are estrogen receptor (ER) -positive and -negative, respectively (Freake et al., 1981; Keydar et al., 1979). Although recently doubt has been cast on the provenance and veracity of HBL100 as a breast cancer cell line (Lacroix, 2008), the results of the IC_{50} that we obtained in this line are included for completeness and allow comparison with the many other previous studies in that cell line. The SKOV3 cell line is a representative ovarian cancer cell line (Fogh and Orfeo, 1977; Fogh et al., 1977) and the HL-60 line is a myeloid leukemia line (Gallagher et al., 1979). All of these lines have abnormal karyotypes and are tumorigenic in nude mice. As a comparison, we also chose to investigate cylinder properties in MRC5 cells derived from human fetal lung tissue that has a normal 2n = 46 karyotype (Jacobs, 1966; Jacobs et al., 1970). This is a nonimmortalized line capable of approximately 42–46 population doublings before senescence.

Cell Culture

All adherent cell lines were routinely cultured in T_{25} flasks (Nunc) at 37°C in a humidified, 5% CO_2 atmosphere, and maintained as a monolayer in Dulbecco's modified Eagle medium supplemented with 10% fetal bovine serum, 2 mM L-glutamine, 100 U ml^{-1} penicillin, and 0.1 mg ml^{-1} streptomycin. The suspension cell line HL-60 was cultured in RPMI medium supplemented in the same manner. Cells were subcultured twice weekly using a standard trypsin-EDTA protocol with the exception of HL-60 cells, which were split

every 2 days. Prior to commencement of experiments, cells were subcultured into 6-well (or 96-well for the MTT assay) culture plates.

MTT Assay and Cellular Growth Assay

The MTT assay (used to determine mitochondrial reductive function and therefore an indicator of cell viability) was utilized to identify the LC_{50} concentrations of iron cylinder $[Fe_2L_3]^{4+}$ and cisplatin. Briefly, cells (10,000 per well or 20,000 cells per well for the T47D cell line) were seeded in a 96-well culture plate (Costar). After a 24 hr period for attachment, cells were incubated in the continuous presence of freshly prepared iron cylinder (0–129 μM) or cisplatin (0–100 μM) for 72 hr. Following treatment, cells were washed with PBS and media were replaced with MTT (0.45 mg ml^{-1}) containing growth media and subsequently incubated at 37°C for 3 hr. Media were aspirated before the addition of DMSO to solubilize the blue formazan product. Culture plates were gently rocked for 1 hr before the absorbance was determined at 530 nm against a DMSO blank. For the cellular proliferation assay, cells (40,000 per well) were seeded in 6-well culture plates (Costar). After an initial 3 hr period for settlement, cells were incubated in the continuous presence of freshly prepared iron cylinder (0–72 μM) or cisplatin (0–5 μM) and cell numbers were calculated every 24 hr for a 6 day period using an improved Neubauer hemocytometer (Hawksley Medical and Laboratory Equipment) following trypsinization of cells where necessary.

Cell-Cycle Analysis

Cells were seeded at 2.5 × 10^5/ml in 4 ml cultures and were treated with and without 10 or 25 μM iron cylinder $[Fe_2L_3]^{4+}$. At the appropriate time points, a 200 μl sample was centrifuged at 500 × g, the supernatant was removed, and 500 μl of cell-cycle buffer (10 μg ml^{-1} propidium iodide, 10^{-4} M sodium chloride, 1% Triton X-100 in distilled water) was added. Following vortexing, samples were stored at 4°C protected from light and were analyzed by flow cytometry on a FACS calibur (Becton Dickinson) on 10,000 events, within 48 hr.

Assessment of Apoptosis by Annexin-V/PI Staining

Cells were seeded at 2.5 × 10^5/ml in 4 ml cultures and were treated with and without 10 or 25 μM iron cylinder $[Fe_2L_3]^{4+}$. At the appropriate time points, a 200 μl sample was stained using an annexin-V FITC kit (Becton Dickinson) according to the manufacturer's instructions. Binding of annexin-V and uptake of propidium iodide were analyzed by flow cytometry of 10,000 events on a Becton Dickinson FACS Calibur utilizing Cell Quest Pro software (Becton Dickinson). The lower left quadrant shows viable cells, lower right indicates cells in early stages of apoptosis, upper right is indicative of late apoptosis, and upper left shows necrotic events.

Propidium Iodide Displacement Assay

The fluorescence spectra for the PI displacement experiment were recorded on a Shimadzu RF-5301 PC fluorescence spectrophotometer (λ_{exc} = 535 nm; range emission = 580–800 nm; resolution = 0.4 nm; speed = medium; excitation split = 10; emission split = 1.5). Solutions of PI (15 or 1.5 μM), ct-DNA (12, 1.2, or 6 μM), NaCl (50 mM), and sodium cacodylate buffer (1 mM) were prepared, measured, and tritiated with iron parent cylinder from ratios of PI:iron cylinder of 200:1 to 4:1, keeping the concentration of PI and ct-DNA constant.

Whole-Cell Hoechst Displacement Assay

The following procedure was that described in Matsuba et al. (2000). HL-60 cells were preincubated with 10 μM Hoechst 33258 in 0.5 ml culture medium at 37°C for 20 min. The iron cylinder was then added (concentrations between 0.1 and 100 μM) followed by a further 20 min incubation at 37°C. Cells were then collected, washed once with chilled PBS, resuspended in chilled PBS, and the fluorescence measured. Fluorescence spectra were recorded in a PTIA fluorescence system. The illumination source was a PTI L-201M using a 75W xenon arc lamp. The detection system was a Shimadzu R298 PMT in a PTI model analog/photon-counting photomultiplier (λ_{exc} = 350 nm; range emission = 380–600 nm; speed = 3 nm/s; excitation split = 5; emission split = 1.5).

DNA Diffusion Assay

As a further assessment of apoptosis, the DNA diffusion assay as described previously (Singh, 2000) was carried out. This assay measures DNA fragmentation as a result of endonuclease activation, one of the final stages of apoptosis. In contrast, annexin-V staining (assessing the presence of phosphatidyl serine in the outer cytoplasmic membrane) is a relatively early temporal marker for apoptosis. Following treatment with iron cylinder $[Fe_2L_3]^{4+}$ at different concentrations, cells (approximately 0.5 × 10^6) were collected by centrifugation (8000 rpm, 3 min), the media were removed, and cell pellets were resuspended in 150 μl of PBS. An aliquot of resuspended cells (15 μl) was placed in a sterile tube containing low-melting-point agarose (150 μl), and this cell suspension was transferred to a glass microscope slide (150 μl per slide; BDH) precoated with 0.5% normal melting-point agarose. Glass coverslips (BDH) were added and slides were placed on a metal tray over ice for 10 min. Coverslips were removed and slides were incubated for 1 hr at 4°C in lysis buffer (2.5 M NaCl, 0.1 M Na_2EDTA, 10 mM Tris base, 1% sodium N-lauryl sarcosinate, 10% DMSO, 1% Triton X-100). Slides were incubated in alkaline solution (75 mM NaOH, 0.2% [v/v] DMSO) for 10 min. Slides were then incubated in ethanol containing 1 M ammonium acetate for 15 min. Next, slides were incubated sequentially for 15 min with 75% ethanol and neutralization buffer (0.4 M Tris, adjusted to pH 7.5). Finally, slides were stained with 50 μl of Sybr Gold (Invitrogen; 10× solution). Slides were examined at 320× magnification using a fluorescence microscope (Zeiss Axiovert 10) fitted with a 450–490 nm excitation filter and a barrier of 520 nm. For each slide, 300 nuclei were scored and the number of apoptotic cells was expressed as a percentage of the total cells scored.

Comet Assay for DNA Strand Breaks

This method was based on that of Singh et al. (1988) as modified in our laboratory (Lee et al., 2005). Following the appropriate treatment at different concentrations of compound for 24 hr, cells were washed in cold PBS and gently scraped into fresh PBS (1 ml). Cells were centrifuged (200 × g, 5 min) and pellets were resuspended in PBS (150 μl). An aliquot of resuspended cells (15 μl) was placed in a sterile tube containing low-melting-point agarose (150 μl), and this cell suspension was transferred to a glass microscope slide (150 μl per slide; BDH) precoated with 0.5% normal melting-point agarose. Glass coverslips (BDH) were added and slides were placed on a metal tray over ice for 10 min. Coverslips were removed and slides were incubated for 1 hr at 4°C in lysis buffer (2.5 M NaCl, 0.1 M Na_2EDTA, 10 mM Tris base, 1% sodium N-lauryl sarcosinate, 10% DMSO, 1% Triton X-100). Following lysis, slides were transferred to a horizontal electrophoresis tank (Pharmacia Biotech) containing electrophoresis buffer (75 mM NaOH, 1 mM Na_2EDTA [pH ~12.8]) and DNA was allowed to unwind for 10 min. DNA was subjected to electrophoresis (25 V, 0.8 Vcm^{-1}, 10 min) and slides were neutralized by washing (3 × 5 min) with neutralization buffer (0.4 M Tris, adjusted to pH 7.5). Slides were subsequently stained with 50 μl of Sybr Gold (Invitrogen; 10× solution). The slides were examined at 320× magnification using a fluorescence microscope (Zeiss Axiovert 10) fitted with a 515–560 nm excitation filter and a barrier filter of 590 nm. A USB digital camera (Merlin; Allied Vision Technologies) received the images, which were analyzed using a personal computer-based image analysis system, Comet assay IV (Perceptive Instruments). Images of 100 randomly selected nuclei were analyzed per slide.

Measurement of percent tail DNA (TD %) was chosen to assess the extent of DNA damage, as this has been shown to suffer much less from interrun variation than other Comet parameters because it is independent of electrophoresis voltage and run time (Olive and Durand, 2005). Median values of three separate experiments were analyzed using ANOVA and post hoc Student's t test, as recommended by Duez et al. (2003).

Bacterial Mutagenicity (Ames) Test

Salmonella typhimurium strains TA 98 and TA100 were kindly provided by Professor B.N. Ames (University of California). Sprague-Dawley rat liver S9 (β-naphthoflavone- and phenobarbital-induced) was obtained from Tebu-Bio (http://www.tebu-bio.com/). Master cultures of bacteria were prepared according to the method of Maron and Ames (1983) and the histidine requirement and genotype were confirmed as recommended in this publication. The assay was based on the preincubation protocol of Maron and Ames (1983) and revertant colonies were counted after the plates had been incubated at 37°C in the dark for 24 hr.

ACKNOWLEDGMENTS

We thank the EU for funding (MARCY RTN HPRN-CT-2002-00175; Marie Curie Fellowship MEIF-CT-2005-024818). Shrikant Jondhale, Zoe Pikramenou, and Richard Green are kindly acknowledged for their help and advice on aspects

of this study. N.J.H. is the recipient of an AstraZeneca-funded molecular toxicology fellowship.

Received: July 4, 2008
Revised: October 6, 2008
Accepted: October 23, 2008
Published: December 19, 2008

REFERENCES

Aung, L., Gorlick, R.G., Shi, W., Thaler, H., Shorter, N.A., Healey, J.H., Huvos, A.G., and Meyers, P.A. (2002). Second malignant neoplasms in long-term survivors of osteosarcoma: Memorial Sloan-Kettering Cancer Center Experience. Cancer *95*, 1728–1734.

Baraldi, P.G., Bovero, A., Fruttarolo, F., Preti, D., Tabrizi, M.A., Pavani, M.G., and Romagnoli, R. (2004). DNA minor groove binders as potential antitumor and antimicrobial agents. Med. Res. Rev. *24*, 475–528.

Cerasino, L., Hannon, M.J., and Sletten, E. (2007). DNA three-way junction with a dinuclear iron(II) supramolecular helicate at the center: a NMR structural study. Inorg. Chem. *46*, 6245–6251.

Charbonniere, L.J., Williams, A.F., Piguet, C., Bernardinelli, G., and Rivara-Minten, E. (1998). Structural, magnetic, and electrochemical properties of dinuclear triple helices: comparison with their mononuclear analogues. Chem. Eur. J. *4*, 485–493.

Childs, L.J., and Hannon, M.J. (2004). Helices and helicates. Supramol. Chem. *16*, 7–22.

Cohen, S.M., and Lippard, S.J. (2001). Cisplatin: from DNA damage to cancer therapy. Prog. Nucleic Acid Res. Mol. Biol. *67*, 93–130.

Da Ros, T., Spalluto, G., Prato, M., Saison-Behmoaras, T., Boutorine, A., and Cacciari, B. (2005). Oligonucleotides and oligonucleotide conjugates: a new approach for cancer treatment. Curr. Med. Chem. *12*, 71–88.

Dervan, P.B. (2001). Molecular recognition of DNA by small molecules. Bioorg. Med. Chem. *9*, 2215–2235.

Duez, P., Dehon, G., Kumps, A., and Dubois, J. (2003). Statistics of the Comet assay: a key to discriminate between genotoxic effects. Mutagenesis *18*, 159–166.

Escudero, M.C., Lassaletta, A., Sevilla, J., Fernandez-Plaza, S., Pérez, A., Diaz, M.A., and Madero, L. (2004). Chemotherapy-related secondary acute myeloid leukemia in patients diagnosed with osteosarcoma. J. Pediatr. Hematol. Oncol. *26*, 454–456.

Fadeel, B., and Orrenius, S. (2005). Apoptosis: a basic biological phenomenon with wide-ranging implications in human disease. J. Intern. Med. *6*, 479–517.

Fisher, D.M., Bednarski, P.J., Grunert, R., Turner, P., Fenton, R.R., and Aldrich-Wright, J.R. (2007). Chiral platinum(II) metallointercalators with potent in vitro cytotoxic activity. ChemMedChem *2*, 488–495.

Fogh, J., and Orfeo, T. (1977). One hundred and twenty seven cultured human tumour cell lines producing tumours in nude mice. J. Natl. Cancer Inst. *59*, 221–226.

Fogh, J., Wright, W., and Loveless, J. (1977). Absence of HeLa cell contamination in 169 cell lines derived from human tumours. J. Natl. Cancer Inst. *58*, 209–214.

Freake, H., Marcocci, C., Iwasaki, J., and MacIntyre, I. (1981). 1,25-dihydroxyvitamin D3 specifically binds to a human breast cancer cell line (T47D) and stimulates growth. Biochem. Biophys. Res. Commun. *101*, 1131–1138.

Gallagher, R., Collins, S., Trujillo, J., McCredie, K., Ahearn, M., Tsai, S., Metzgar, R., Aulakh, G., Ting, R., Ruscett, F., and Gallo, R. (1979). Characterization of the continuous, differentiating myeloid cell line (HL-60) from a patient with acute promyelocytic leukemia. Blood *54*, 713–733.

Gebel, T., Lantzsch, H., Plessow, K., and Dunkelberg, H. (1997). Genotoxicity of platinum and palladium compounds on human and bacterial cells. Mutat. Res. *389*, 183–190.

Guo, Z.J., and Sadler, P.J. (2000). Medicinal inorganic chemistry. Adv. Inorg. Chem. *49*, 183–306.

Hannon, M.J. (2007a). Supramolecular DNA recognition. Chem. Soc. Rev. *36*, 280–295.

Hannon, M.J. (2007b). Metal-based anticancer drugs: from a past anchored in platinum chemistry to a post-genomic future of diverse chemistry and biology. Pure Appl. Chem. *79*, 2243–2261.

Hannon, M.J., Moreno, V., Prieto, M.J., Molderheim, E., Sletten, E., Meistermann, I., Isaac, C.J., Sanders, K.J., and Rodger, A. (2001a). Intramolecular DNA coiling mediated by a metallo-supramolecular cylinder. Angew. Chem. Int. Ed. Engl. *40*, 879–884.

Hannon, M.J., Meistermann, I., Isaac, C.J., Blomme, C., Rodger, A., and Aldrich-Wright, J.R. (2001b). A cheap yet effective chiral stationary phase for chromatographic resolution of metallo-supramolecular helicates. Chem. Commun., 1078–1079.

Harris, A.L., Yang, X., Hegmans, A., Povirk, L., Ryan, J., Kelland, L., and Farrell, N.P. (2005a). Synthesis, characterization, and cytotoxicity of a novel highly charged trinuclear platinum compound. Enhancement of cellular uptake with charge. Inorg. Chem. *44*, 9598–9600.

Harris, A.L., Ryan, J.J., and Farrell, N.P. (2005b). Biological consequences of trinuclear platinum complexes: comparison of [{trans-PtCl$(NH_3)_2$}2μ-(trans-Pt$(NH_3)_2(H_2N(CH_2)_6$-$NH_2)_2$)]$^{4+}$ (BBR 3464) with its noncovalent congeners. Mol. Pharmacol. *69*, 666–672.

Heffeter, P., Jakupec, M.A., Korner, W., Wild, S., von Keyserlingk, N.G., Elbling, L., Zorbas, H., Korynevska, A., Knasmuller, S., Sutterluty, H., et al. (2006). Multidrug-resistant cancer cells are preferential targets of the new antineoplastic lanthanum compound KP772 (FFC24). Biochem. Pharmacol. *71*, 426–440.

Hotze, A.C.G., van der Geer, E.P.L., Kooijman, H., Spek, A.J., Haasnoot, J.G., and Reedijk, J. (2005). Characterization by NMR spectroscopy, X-ray analysis and cytotoxic activity of the ruthenium(II) compounds [RuL_3]$(PF6)_2$(L = 2-phenylazopyridine or o-tolylazopyridine) and [RuL′2L″]$(PF6)_2$(L′, L″ = 2-phenylazopyridine, 2,2′-bipyridine). Eur. J. Inorg. Chem. *2005*, 2648–2657.

Hotze, A.C.G., Kariuki, B.M., and Hannon, M.J. (2006). Dinuclear double-stranded metallosupramolecular ruthenium complexes: potential anticancer drugs. Angew. Chem. Int. Ed. Engl. *45*, 4839–4842.

Jacobs, J.P. (1966). A simple medium for the propagation and maintenance of human diploid cell strains. Nature *210*, 100–101.

Jacobs, J.P., Jones, C., and Baille, J.P. (1970). Characteristics of a human diploid cell designated MRC-5. Nature *227*, 168–170.

Kerckhoffs, J.M.C.A., Peberdy, J.C., Meistermann, I., Childs, L.J., Isaac, C.J., Pearmund, C.R., Reudegger, V., Khalid, S., Alcock, N.W., Hannon, M.J., and Rodger, A. (2007). Enantiomeric resolution of supramolecular helicates with different surface topographies. Dalton Trans. 734–742.

Keydar, I., Chen, L., Karby, S., Weiss, F., Delarea, J., Radu, M., Chaitcik, S., and Brenner, H. (1979). Establishment and characterization of a cell line of human breast carcinoma origin. Eur. J. Cancer *15*, 659–670.

Khalid, S., Hannon, M.J., Rodger, A., and Rodger, P.M. (2006). Simulations of DNA coiling around a synthetic supramolecular cylinder that binds in the DNA major groove. Chem. Eur. J. *12*, 3493–3506.

Komeda, S., Moulaei, T., Woods, K., Chikuma, M., Farrell, N.P., and Williams, L.D. (2006). A third mode of DNA binding: phosphate clamps by a polynuclear platinum complex. J. Am. Chem. Soc. *128*, 16092–16103.

Kramer, R., Lehn, J.M., DeCian, A., and Fischer, J. (1993). Self-assembly, structure and spontaneous resolution of a trinuclear triple-helix form an oligobipyridine ligand and Ni(II) ions. Angew. Chem. Int. Ed. Engl. *32*, 703–706.

Lacroix, M. (2008). Persistent use of "false" cell lines. Int. J. Cancer *122*, 1–4.

Lee, A.J., Hodges, N.J., and Chipman, J.K. (2005). Interindividual variability in response to sodium dichromate-induced oxidative DNA damage: role of the Ser326Cys polymorphism in the DNA-repair protein of 8-oxo-7,8-dihydro-2′-deoxyguanosine DNA glycosylase 1 (OGG1). Cancer Epidemiol. Biomarkers Prev. *14*, 497–505.

Lincoln, P., and Nordén, B. April 1999. Binuclear complex. Patent PCT/SE98/01655.

Lippert, B., ed. (1999). Cisplatin: Chemistry and Biochemistry of a Leading Anticancer Drug (Weinheim, Germany: Wiley-VCH).

Malina, J., Hannon, M.J., and Brabec, V. (2007). Recognition of DNA three-way junctions by metallosupramolecular cylinders: gel electrophoresis studies. Chem. Eur. J. *13*, 3871–3877.

Maron, D.M., and Ames, B.N. (1983). Revised methods for the Salmonella mutagenicity test. Mutat. Res. *113*, 173–215.

Martínez, R., and Chacón-García, L. (2005). The search of DNA-intercalators as antitumoral drugs: what worked and what did not work. Curr. Med. Chem. *12*, 127–151.

Matsuba, Y., Edatsugi, E., Mita, I., Matsunaga, A., and Nakanishi, O. (2000). A novel synthetic DNA minor groove binder, MS-247: antitumor activity and cytotoxic mechanism. Cancer Chemother. Pharmacol. *46*, 1–9.

Meistermann, I., Moreno, V., Prieto, M.J., Moldrheim, E., Sletten, E., Khalid, S., Rodger, P.M., Peberdy, J.C., Isaac, C.J., Rodger, A., and Hannon, M.J. (2002). Intramolecular DNA coiling mediated by metallo-supramolecular cylinders: differential binding of P and M helical enantiomers. Proc. Natl. Acad. Sci. USA *99*, 5069–5074.

Moldrheim, E., Hannon, M.J., Meistermann, I., Rodger, A., and Sletten, E. (2002). Interaction between a DNA oligonucleotide and a dinuclear iron(II) supramolecular cylinder; an NMR and molecular dynamics study. J. Biol. Inorg. Chem. *7*, 770–780.

Nielsen, P.E. (2001). Targeting double stranded DNA with peptide nucleic acid (PNA). Curr. Med. Chem. *8*, 545–550.

Oleksi, A., Blanco, A.G., Boer, R., Uson, I., Aymami, J., Rodger, A., Hannon, M.J., and Coll, M. (2006). Molecular recognition of a three-way DNA junction by a metallosupramolecular helicate. Angew. Chem. Int. Ed. Engl. *45*, 1227–1231.

Olive, P.L., and Durand, R.E. (2005). Heterogeneity in DNA damage using the Comet assay. Cytometry A *66*, 1–8.

Önfelt, B., Göstring, L., Lincoln, P., Nordén, P., and Önfelt, A. (2002). Cell studies of the DNA bis-intercalator δ-δ [μ-C4(cpdppz)(2)-(phen)(4)Ru(2)](4+): toxic effects and properties as a light emitting DNA probe in V79 Chinese hamster cells. Mutagenesis *17*, 317–320.

Pascu, G.I., Hotze, A.C.G., Sanchez Cano, C., Kariuki, B.M., and Hannon, M.J. (2007). Dinuclear ruthenium(II) triple-stranded helicates: luminescent supramolecular cylinders that bind and coil DNA and exhibit activity against cancer cell lines. Angew. Chem. Int. Ed. Engl. *46*, 4374–4378.

Peberdy, J.C., Malina, J., Khalid, S., Hannon, M.J., and Rodger, A. (2007). Influence of surface shape on DNA binding of bimetallo helicates. J. Inorg. Biochem. *101*, 1937–1945.

Reedijk, J. (1996). Improved understanding in platinium antitumour chemistry. Chem. Commun. 801–806.

Singh, N.P. (2000). A simple method for accurate estimation of apoptotic cells. Exp. Cell Res. *256*, 328–337.

Singh, N.P., McCoy, M.T., Tice, R.R., and Schneider, E.L. (1988). A simple technique for quantitation of low levels of DNA damage in individual cells. Exp. Cell Res. *175*, 184–191.

Takahara, P.M., Rosenzweig, A.C., Frederick, C.A., and Lippard, S.J. (1995). Crystal structure of double-stranded DNA containing the major adduct of the anticancer drug cisplatin. Nature *377*, 649–652.

Thuong, N.T., and Helene, C. (1993). Sequence-specific recognition and modification of double-helical DNA by oligonucleotides. Angew. Chem. Int. Ed. Engl. *32*, 666–690.

Uno, Y., and Morita, M. (1993). Mutagenic activity of some platinum and palladium complexes. Mutat. Res. *298*, 269–275.

Wang, X., Cheung, H.W., Chun, A.C., Jin, D.Y., and Wong, Y.C. (2008). Mitotic checkpoint defects in human cancers and their implications to chemotherapy. Front. Biosci. *13*, 2103–2114.

Wheate, N.J., Brodie, C.R., Collins, J.G., Kemp, S., and Aldrich-Wright, J.R. (2007). DNA intercalators in cancer therapy: organic and inorganic drugs and their spectroscopic tools of analysis. Mini Rev. Med. Chem. *7*, 627–648.

Wierecky, J., Kollmannsberger, C., Boehlke, I., Kuczyk, M., Schleicher, J., Schleucher, N., Metzner, B., Kanz, L., Hartmann, J.T., and Bokemeyer, C. (2005). Secondary leukemia after first-line high-dose chemotherapy for patients with advanced germ cell cancer. J. Cancer Res. Clin. Oncol. *131*, 255–260.